

## Implications of Mean Intracellular Water Lifetime for Prostate DCE-MRI Modeling

X. Li<sup>1</sup>, R. A. Priest<sup>2,3</sup>, W. J. Woodward<sup>1</sup>, I. J. Tagge<sup>1</sup>, F. Siddiqui<sup>2,3</sup>, T. M. Beer<sup>4,5</sup>, M. G. Garzotto<sup>6,7</sup>, W. Huang<sup>1</sup>, W. D. Rooney<sup>1</sup>, and C. S. Springer, Jr.<sup>1,5</sup>

<sup>1</sup>Advanced Imaging Research Center, Oregon Health & Science University, Portland, Oregon, United States, <sup>2</sup>Radiology, Oregon Health & Science University, Portland, Oregon, United States, <sup>3</sup>School of Medicine, Oregon Health & Science University, Portland, Oregon, United States, <sup>4</sup>Hematology/Oncology, Oregon Health & Science University, Portland, Oregon, United States, <sup>5</sup>Knight Cancer Institute, Oregon Health & Science University, Portland, Oregon, United States, <sup>6</sup>Urology, Oregon Health & Science University, Portland, Oregon, United States, <sup>7</sup>Portland VA Medical Center, Portland, Oregon, United States

**Introduction:** In standard modeling (SM) of Dynamic-Contrast-Enhanced MRI (DCE-MRI) pharmacokinetics (1), it is assumed that inter-compartmental water exchange kinetics are always effectively infinitely fast. Though it is physically impossible that such processes be truly infinitely rapid, in many tissue regions they seem so as far as DCE-MRI  $^1\text{H}_2\text{O}$  signals are concerned: the exchange MR systems remain in their fast-exchange-limit [FXL] conditions. However, there are tissue *loci* where systems transiently depart their FXLs during DCE-MRI contrast reagent (CR) bolus passage (2). In such a case, the mean ROI or voxel intracellular water lifetime ( $\tau_i$ ) can become estimable. The smaller the  $\tau_i$  value the more this requires tissues, like prostate, featuring extensive CR extravasation - a large  $K^{\text{trans}}$  extravasation rate constant. Information gained can be very useful since  $\tau_i$  is directly tied to the cellular physiological properties: membrane water permeability coefficient,  $P_w$  (3), energetic state (4), and size. Using an exchange-sensitized DCE-MRI acquisition and analytical model, prostate  $\tau_i$  maps have been obtained. These provide new clinical insights.

**Methods:** Prostate  $^1\text{H}_2\text{O}$  MRI data were acquired on 13 subjects with a Siemens TIM Trio (3T) system under an IRB-approved protocol. RF transmitting was through the whole body coil and RF receiving was with a combination of Spine Matrix and flexible Body Matrix coil arrays. The DCE-MRI acquisition employed a 3D TurboFLASH pulse sequence with a 256\*144\*16 matrix size and a 360\*203 mm<sup>2</sup> FOV, resulting in (1.4)<sup>2</sup> mm<sup>2</sup> in-plane resolution. Other parameters are: slice thickness: 3 or 3.2 mm; TR/TE/FA: 5.0 ms/1.57 ms/15°, inter-image sampling interval: 6.3 s. A 0.1 mmol/kg CR (Prohance; Bracco) bolus was administered starting ~30 s after commencing the DCE-MRI sequence. Other details are given in (5). All subjects subsequently underwent standard ten-core prostate biopsies with ultrasound guidance. DCE data were analyzed using the first generation shutter-speed model (SSM1), which focuses on cell membrane water exchange kinetics and allows  $\tau_i$  estimation (1). For prostate tissue,  $\tau_i$  is often the 3<sup>rd</sup> most sensitive parameter (after  $K^{\text{trans}}$ , and  $v_e$ , the extracellular extravascular volume fraction) (6), even more sensitive than the blood volume fraction.

**Results:** Figure 1 shows  $\tau_i$  color maps overlaid on a central set of nine post-contrast axial pelvic DCE image slices of a subject. No malignancy was found in the subsequent biopsy specimens. Conspicuous peripheral/central zone contrast is evident in most slices. Many transitional/central zone pixels have very small  $\tau_i$  values - essentially zero. Of course, no  $\tau_i$  is actually zero: but  $\tau_i$  must be quite small in these areas because it is precisely these exhibiting the largest  $K^{\text{trans}}$  values (5), see below. Either the cell membranes have large passive (3) or active (4)  $P_w$  values, their sizes are small, or some combination of these. The  $\tau_i$  values for a majority of peripheral zone (and possibly fibromuscular stroma) pixels are in the 300-800 ms range. From literature physiological NMR studies (3) where  $\tau_i$  can be measured with greater precision, this is very reasonable and supports the  $\tau_i$  parameter interpretation. The (spatial) correlation with known tissue structure (*i.e.*, peripheral zone) supports  $\tau_i$  significance. This suggests that peripheral zone cell membrane water exchange systems depart their FXLs during the CR passage, but transitional/central zone systems generally do not. In general, the use of SM analysis in cases such as the former can lead to systematic errors in other DCE-MRI parameters ( $K^{\text{trans}}$  and  $v_e$ ). SM has no provision for transient FXL departure, and has to put its consequence in one or both parameter values. SM should be employed only if the DCE-MRI data are collected in an exchange-minimized acquisition (7). However, besides precluding access to  $\tau_i$ , the latter also incurs a significant signal to noise ratio (SNR) penalty. For prostate MRI, where endorectal RF receive coils are usually employed to boost SNR, an exchange-minimized data acquisition is counterproductive.

A consequence of FXL-departure on disease visualization is shown in Figure 2. This is a subject whose surgical pathology report indicated adenocarcinoma in four-core biopsy samples from the left prostate base, left mid prostate, and left prostate apex. Parametric  $K^{\text{trans}}$ (SM) and  $K^{\text{trans}}$ (SSM) maps are shown in panels **a** and **b**. First, we note the aforementioned fact (5) that normal-appearing tissue  $K^{\text{trans}}$  values are largest (0.35 min<sup>-1</sup> is very large) in the transitional/central zone region: the low  $\tau_i$  values seen in this area (panel **d**) must be truly small. Though it is not obvious with this color scale, the normal-appearing peripheral zone (image left)  $K^{\text{trans}}$  values ( $\geq 0.1$  min<sup>-1</sup>) are large enough to reveal normal-sized  $\tau_i$  values. Second, the "hot spot" seen on the left side of the prostate (image right) is concordant with the pathology finding of cancer. In this, the  $K^{\text{trans}}$  values ( $> 0.8$  min<sup>-1</sup>) are quite large. However, the diameter of maximum  $K^{\text{trans}}$ (SSM) is greater than that of  $K^{\text{trans}}$ (SM) in the hot spot. This is most evident in the panel **c**  $\Delta K^{\text{trans}}$  map [=  $K^{\text{trans}}$ (SSM) -  $K^{\text{trans}}$ (SM)]: a very clear rim enhancement is visible. The SM is underestimating  $K^{\text{trans}}$  (relative to the SSM) in the tumor rim. Since the only difference in the SSM and SM analyses lies precisely in their cell membrane water exchange treatments, this clearly suggests transient FXL-departure in the rim voxels. This is further supported in the panel **d**  $\tau_i$  map, which also exhibits tumor rim enhancement, as well as the normal-appearing peripheral zone enhancement. We have seen ring enhancement patterns also in other malignant cases. The very small  $\tau_i$  values in the tumor core must be truly small (suggesting necrosis) because the associated  $K^{\text{trans}}$  values are very large.

**Discussion:** For this small subject group, we were able to obtain  $\tau_i$  maps without using an endorectal RF coil. It appears that the  $\tau_i$  value can change with pathology and could provide insights not previously available. It should be noted that we see  $\Delta K^{\text{trans}}$  map rim enhancement only when the SSM1 model is employed: not with the SSM2 model. Since this seems clearly to have anatomical significance, it provides further evidence of disproportionate transverse relaxation compartmental  $^1\text{H}_2\text{O}$  signal "quenching" in DCE-MRI (3). With new acquisition pulse sequences [such as TWIST (Siemens)] enabling high spatiotemporal resolution DCE-MRI, multi-slice parametric mapping will become more practical and allow for even more exchange-sensitive data acquisitions.

**Grant Support:** NIH: RO1-EB00422, RO1-NS40801, Medical Research Foundation of Oregon.

**Reference:** 1. Tofts, Brix, Buckley, *et al. J Magn Reson Imaging*, 10:223-232 (1999). 2. Yankeelov, Rooney, Li, Springer *Magn Reson Med.* **50**:1151-1169 (2003). 3. Li, Huang, Morris, *et al. Proc Natl Acad Sci* 2008;105:17937-17942. 4. Zhang, Poirier-Quintin, Springer, Balschi, *Proc. Int Soc Magn Reson Med.* **17**: 3150 (2009). 5. Priest, Li, Tagge, Woodward, Beer, Springer, Garzotto, *Proc. Int Soc Magn Reson Med.* **18**: 2809 (2010). 6. Li, Rooney, Springer, *Proc. Int Soc Magn Reson Med.* **18**: 3392 (2010). 7. Bains, McGrath, Naish, Cheung, Watson, Taylor, Logue, Parker, Waterton, Buckley, *Magn Reson Med.* **64**: 595- 603 (2010).

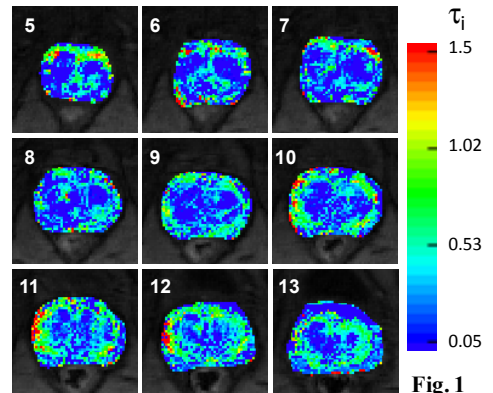


Fig. 1

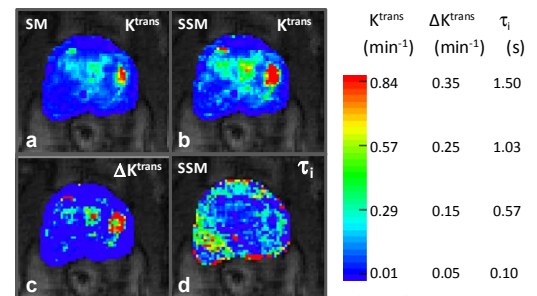


Figure 2.